PHYSICAL MATERIALS TECHNOLOGY

Original article
DOI: https://doi.org/10.18721/JPM.18207

POLYCRYSTALLINE FILMS OF $MA_xMEA_{1-x}PBI_3$ HYBRID PEROVSKITES OBTAINED BY THE SOLUTION METHOD: CRYSTALLIZATION AND MORPHOLOGY

A. A. Ryabko[1], *M. K. Ovezov*[1]✉, *A. I. Maximov*[2], *N. V. Permiakov*[2], *A. K. Tuchkovskiy*[3], *I. A. Vrublevskiy*[3], *E. N. Muratova*[2], *A. N. Aleshin*[1], *V. A. Moshnikov*[2]

[1] Ioffe Institute of RAS, St. Petersburg, Russia;

[2] St. Petersburg Electrotechnical University "LETI", St. Petersburg, Russia;

[3] Belarusian State University of Informatics and Radioelectronics, Minsk, Republic of Belarus

✉ strontiumx94@gmail.com

Abstract. In this work, the morphological features of polycrystalline films of hybrid perovskites $MA_xMEA_{1-x}PbI_3$ formed by a single-stage centrifugation method from DMF and DMSO solutions (4:1) have been investigated. The results of the studies showed that an increase in the proportion of monoethanolammonium in $MA_xMEA_{1-x}PbI_3$ led not only to a change in the absorption spectra and an increase in the interplanar distances of the crystal lattice, but also to a significant change in the morphology of the films from elongated split crystallites to a uniform coating of nanocrystallites. An increase in the proportion of monoethanolammonium iodide in the solution also improved the wettability of solutions and the continuity of the coating of substrates with hybrid perovskite $MA_xMEA_{1-x}PbI_3$ without additional surface activation processes. The increased band gap of $MA_xMEA_{1-x}PbI_3$ compared to $MAPbI_3$ makes these hybrid perovskites attractive for use in tandem solar cells.

Keywords: hybrid perovskites, polycrystalline film, solar cell, split crystallite, morphology, crystallization

Funding: The work was carried out with the support of a grant from Russian Science Foundation No. 23-42-10029 dated 20 December 2022, https://rscf.ru/en/project/23-42-10029/. This research was funded by the Belarusian Republican Foundation for Fundamental Research grant number F23RNF-160.

Citation: Ryabko A. A., Ovezov M. K., Maximov A. I., Permiakov N. V., Tuchkovskiy A. K., Vrublevskiy I. A., Muratova E. N., Aleshin A. N., Moshnikov V. A., Polycrystalline films of $MA_xMEA_{1-x}PbI_3$ hybrid perovskites obtained by the solution method: Crystallization and morphology, St. Petersburg State Polytechnical University Journal. Physics and Mathematics. 18 (2) (2025) 69–81. DOI: https://doi.org/10.18721/JPM.18207

Научная статья
УДК 538.91
DOI: https://doi.org/10.18721/JPM.18207

КРИСТАЛЛИЗАЦИЯ И МОРФОЛОГИЯ ПОЛИКРИСТАЛЛИЧЕСКИХ ПЛЕНОК ГИБРИДНЫХ ПЕРОВСКИТОВ $MA_xMEA_{1-x}PBI_3$, ПОЛУЧЕННЫХ РАСТВОРНЫМ МЕТОДОМ

А. А. Рябко[1], *М. К. Овезов*[1]✉, *А. И. Максимов*[2], *Н. В. Пермяков*[2], *А. К. Тучковский*[3], *И. А. Врублевский*[3], *Е. Н. Муратова*[2], *А. Н. Алешин*[1], *В. А. Мошников*[2]

[1] Физико-технический институт имени А. Ф. Иоффе РАН, Санкт-Петербург, Россия;

[2] Санкт-Петербургский государственный электротехнический университет «ЛЭТИ» им. В. И. Ульянова (Ленина), Санкт-Петербург, Россия;

[3] Белорусский государственный университет информатики и радиоэлектроники, Минск, Республика Беларусь

✉ strontiumx94@gmail.com

Аннотация. В работе были исследованы морфологические особенности поликристаллических пленок гибридных перовскитов $MA_xMEA_{1-x}PbI_3$, сформированных одностадийным методом центрифугирования из растворов ДМФ и ДМСО (4:1). Результаты исследований показали, что увеличение доли моноэтаноламмония в $MA_xMEA_{1-x}PbI_3$ приводит не только к изменению спектров поглощения и увеличению межплоскостных расстояний кристаллической решетки, но также к существенному изменению морфологии пленок от вытянутых расщепленных кристаллитов до однородного покрытия из нанокристаллитов. Увеличение доли моноэтаноламмония йодида в растворе также обеспечивает улучшение смачиваемости растворов и сплошность покрытия подложек гибридным перовскитом $MA_xMEA_{1-x}PbI_3$ без дополнительных процессов активации их поверхности. Увеличенная ширина запрещенной зоны $MA_xMEA_{1-x}PbI_3$, по сравнению с $MAPbI_3$, делает эти гибридные перовскиты привлекательными для использования в тандемных солнечных элементах.

Ключевые слова: гибридные перовскиты, поликристаллическая пленка, солнечный элемент, расщепленный кристаллит, морфология, кристаллизация

Финансирование: Авторы благодарны аспиранту СПбГЭТУ «ЛЭТИ» Корепанову О.А. за измерения рентгенограмм образцов гибридных перовскитов $MA_xMEA_{1-x}PbI_3$. В части синтеза металлоорганических перовскитов работа выполнена при поддержке гранта Белорусского республиканского фонда фундаментальных исследований № Ф23РНФ-160 и Российского научного фонда № 10029-42-23 (https://rscf.ru/project/10029-42-23/) от 20.12.2022.

Ссылка для цитирования: Рябко А. А., Овезов М. К., Максимов А. И., Пермяков Н. В., Тучковский А. К., Врублевский И. А., Муратова Е. Н., Алешин А. Н., Мошников В. А. Кристаллизация и морфология поликристаллических пленок гибридных перовскитов $MA_xMEA_{1-x}PbI_3$, полученных растворным методом // Научно-технические ведомости СПбГПУ. Физико-математические науки. 2025. Т. 18. № 2. С. 69–81. DOI: https://doi.org/10.18721/JPM.18207

Introduction

Materials based on hybrid perovskites are of great interest for applications in photovoltaics and photodetectors, due to their direct-bandgap structure, tunable band gap, high absorption coefficient, high mobility and long mean free path [1, 2]. In addition, hybrid perovskites are promising for creating X-ray detectors, optically-controlled memristors and light-emitting devices [3–5].

A wide range of polycrystalline $APbX_3$-based films is used to create photovoltaic structures, typically with varying proportions of formamidinium (FA^+, $CH(NH_2)_2^+$) and methylammonium (MA^+, $CH_3NH_3^+$) cations and I^-, Br^-, Cl^- anions, as well as by introducing inorganic cations or partial substitution of lead [6–9]. A wide range of hybrid perovskite compositions is also used to fabricate tandem solar cells [10, 11], which is particularly attractive for further development of heterostructure silicon solar cells, where hybrid perovskites with a wider band gap are used. Using complex compositions of hybrid perovskites is aimed at improving stability while ensuring optimal band gap and efficiency for the solar cell [12].

A transition is currently underway from nanotechnology to nanoarchitectonics, providing a synergistic effect from the contact of two nanomaterials [13]. To improve the stability of perovskite photovoltaic structures, molecular etching and growth of films from 3D/2D perovskites are widely used [14–17]. Long-chain amines are commonly used for this purpose, whose $-NH_2$ terminal groups interact with uncoordinated lead ions and passivate defects on the periphery of grains, or, like some short-chain amines, can serve as organic binders between inorganic octahedral frameworks in quasi-2D perovskites [15]. However, some short-chain amines, along with formamidinium and methylammonium cations, can integrate into the crystal lattice of hybrid perovskite with a change in the band gap [18].

The goal of this paper is to identify the effect of the proportion of monoethanolammonium in $MA_xMEA_{1-x}PbI_3$ hybrid perovskite on the crystallization, optical properties, and morphology of polycrystalline films produced by single-stage synthesis from solution.

Experimental

Preparation of solutions. A solution of $MA_xMEA_{1-x}PbI_3$ hybrid perovskite was obtained by mixing a solution of monoethanolammonium iodide $HOCH_2CH_2NH_3I$ (with the concentration of 0.645 mol/l) and lead iodide PbI_2 (with the same concentration, i.e., 0.645 mol/l) with a solution of hybrid perovskite $MAPbI_3$ of equimolar concentration with 1 : 3, 1 : 1 and 3 : 1 volume ratios for varying proportions of the monoethanolammonium cation $HOCH_2CH_2NH_3^+$ (MEA) in the range from 0.25 to 0.75, respectively.

A solution of dimethylformamide (DMFA) with dimethyl sulfoxide (DMSO) with a volume ratio of 4:1 was used as a solvent. DMSO increases the solubility limit of lead iodide [19]. The ratio of DMFA and DMSO was also chosen because the precipitator can be subsequently used successfully for one-step spin-coating [19, 20].

To obtain polycrystalline layers of $MA_xMEA_{1-x}PbI_3$, solutions with a mass concentration of about 400 mg/ml were deposited on glass substrates by spin-coating followed by heating on a laboratory hot plate at 110 °C for 10 minutes. The spin-coating rate was 3000 rpm (for 30 s) with spin-up at 1000 rpm (10 s). Before applying the perovskite films, the glass substrates were thoroughly washed in soap solution, distilled water, acetone and isopropyl alcohol using an ultrasonic bath (10 minutes each). To confirm the formation of the crystalline structure of hybrid perovskites, samples were deposited on glass substrates by drop-casting followed by annealing at 110 °C to obtain thick layers.

Methods. To study the contact angle of $MA_xMEA_{1-x}PbI_3$ solutions in DMFA and DMSO, solutions with a volume of about 5 μl were applied to clean glass substrates and then monitored using an optical microscope.

The morphology of $MA_xMEA_{1-x}PbI_3$ polycrystalline layers was studied using optical microscopy (POLAM-312 polarization microscope) and atomic force microscopy (Ntegra Therma system from NT-MDT).

Optical absorption spectra were measured using a PE-5400UF spectrophotometer. X-ray images were obtained using a Bruker D2 PHASER diffractometer (Bruker, USA) with a scan speed of 1 deg/min with a CuK_α X-ray source.

Results and discussion

Results of X-ray diffraction (XRD) analysis for $MAPbI_3$ and $MA_{0.75}MEA_{0.25}PbI_3$, $MA_{0.5}MEA_{0.5}PbI_3$, $MA_{0.25}MEA_{0.75}PbI_3$ solid solutions (Fig. 1) with intense peaks that were attributed to the (110), (220), (310), (224), (330) planes, and minor peaks of the (200), (202), and (312) planes confirmed the tetragonal structure of perovskite [21]. Furthermore, with an increase in the proportion of monoethanolammonium in the composition of hybrid perovskites, a shift of peaks towards a decrease in the 2Θ angle is observed in the XRD patterns, indicating an increase in the interplanar distances of the crystal lattice.

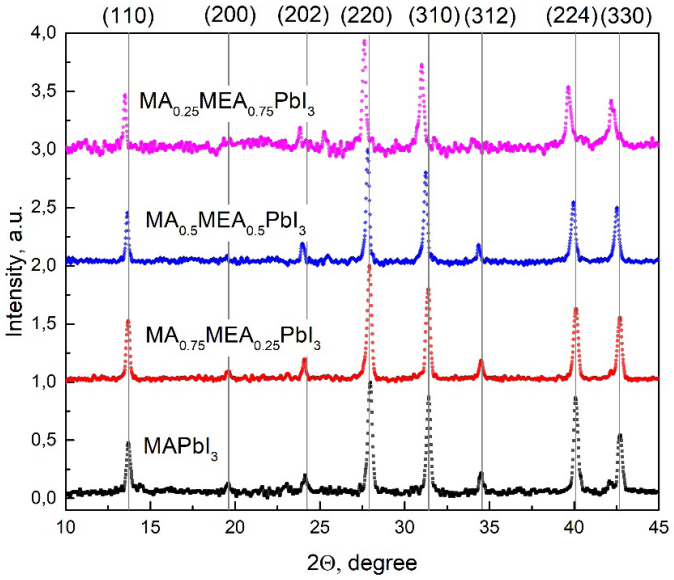

Fig. 1. XRD patterns of obtained materials: $MAPbI_3$ thick films and $MA_{0.75}MEA_{0.25}PbI_3$, $MA_{0.5}MEA_{0.5}PbI_3$, $MA_{0.25}MEA_{0.75}PbI_3$ solid solutions

An increase in the proportion of monoethanolammonium in the composition of $MA_xMEA_{1-x}PbI_3$ hybrid perovskites also leads to a change in the optical absorption spectra of the films. As follows from the spectra in Fig. 2, an increase in the proportion of monoethanolammonium in the composition leads to a shift in its absorption edge to the short-wavelength region, i.e., an increase in the band gap.

Results obtained by XRD analysis and spectrophotometry indicate the incorporation of monoethanolammonium cations into the crystal lattice, which leads to an increase in the interplanar distances in the crystal lattice, an increase in the optical band gap, and a change in absorption spectra with an increase in the proportion of monoethanolammonium in $MA_xMEA_{1-x}PbI_3$ solid solutions. The possibility of increasing the band gap with an increase in the proportion of monoethanolammonium makes $MA_xMEA_{1-x}PbI_3$ solid solutions attractive for use in tandem solar cells.

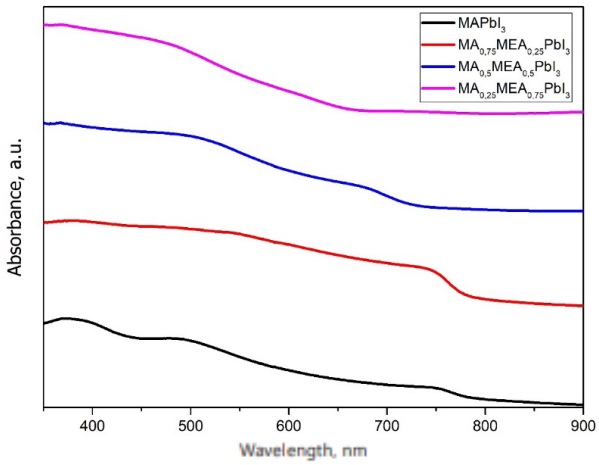

Fig. 2. Normalized optical absorption spectra of $MAPbI_3$ perovskite films and $MA_{0.75}MEA_{0.25}PbI_3$, $MA_{0.5}MEA_{0.5}PbI_3$, $MA_{0.25}MEA_{0.75}PbI_3$ solid solutions

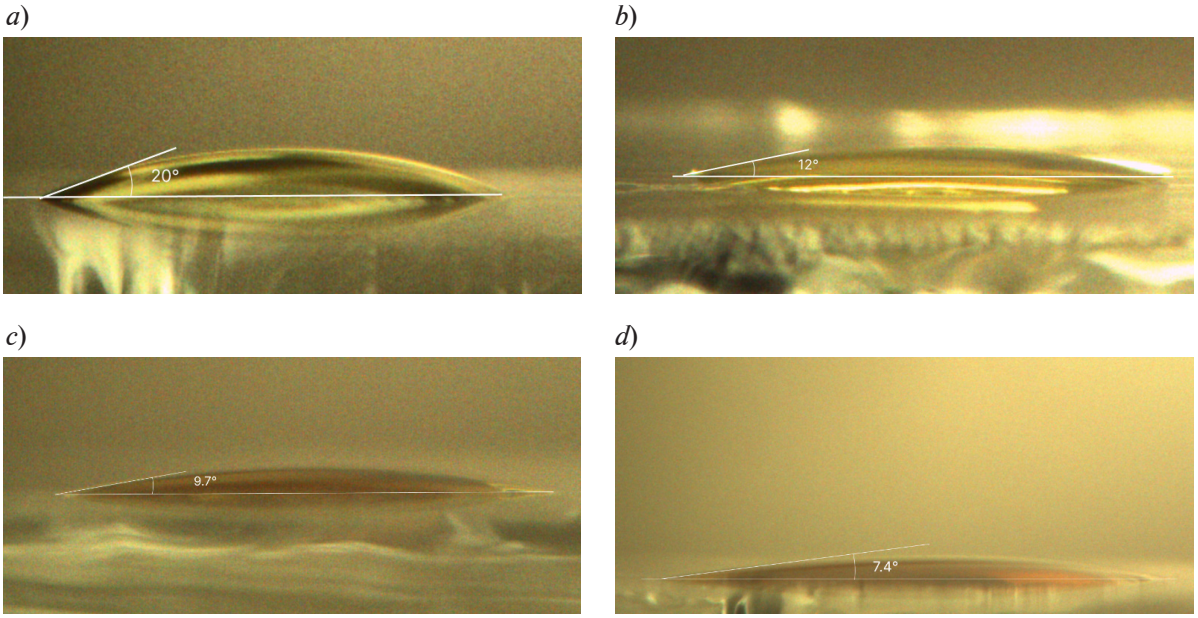

Fig. 3. Measurements of contact angle in hybrid perovskite solutions in DMFA with DMSO from photographs: $MAPbI_3$ (*a*), $MA_{0.75}MEA_{0.25}PbI_3$ (*b*), $MA_{0.5}MEA_{0.5}PbI_3$ (*c*), $MA_{0.25}MEA_{0.75}PbI_3$ (*d*)

The measurement results for contact angles of $MAPbI_3$, $MA_{0.75}MEA_{0.25}PbI_3$, $MA_{0.5}MEA_{0.5}PbI_3$, $MA_{0.25}MEA_{0.75}PbI_3$ compounds in DMFA and DMSO solutions on the surface of glass substrates are shown in Fig. 3.

According to the data in Fig. 3, the $MAPbI_3$ solution shows the largest contact angle, and the 1 : 3 ratio of the MEAI and MAI components in the solution leads to a significant decrease in this angle from about 20° to 12°. Therefore, this ratio makes it possible to improve wettability without introducing significant distortions into the perovskite crystal lattice. A further increase in the proportion of MEAI relative to MAI to a 3 : 1 ratio ensures a further decrease in the contact angle (to about 7.4°). Better wettability of the substrate surface with the solution typically contributes to more uniform coating of the substrate, at both macro and microscales.

The results of optical microscopy studies of $MA_xMEA_{1-x}PbI_3$ perovskite films are shown in Fig. 4. Evidently, elongated split crystallites with a characteristic size of about 25 μm are predominantly formed under these conditions for $MAPbI_3$ film synthesized from solution in DMFA and DMSO (see Fig. 4,*a*). Crystallization of $MA_{0.75}MEA_{0.25}PbI_3$ films leads to the formation of larger elongated split crystallites with characteristic sizes of 0.1–0.2 mm (see Fig. 4,*b*). Such elongated crystallites may be promising for applications in planar structures, for example, photodetectors or X-ray detectors [22], since they likely contain fewer grain boundaries in the lateral direction than polycrystalline films with characteristic crystallite sizes in fractions of micrometers. However, such a crystallization process can be critical for vertical structures, since it can be accompanied by discontinuities in the coating of the substrate surface, uneven thickness and microcavities forming under split crystallites, which can lead to efficiency loss of the device or shunting of the perovskite layer.

As shown in [23], the formation of large elongated crystallites in hybrid perovskites may be associated with homogeneous nucleation in the near-surface region of the thin film of the solution. Evaporation of the solvent leads to an increase in the solute concentration in the near-surface region, and a lower temperature at the surface of the solution layer reduces the solubility of perovskite, providing supersaturation and homogeneous nucleation. A small concentration of nuclei in the near-surface layer and a long evaporation process lead to the formation of large elongated crystallites. Another nucleation region to be considered is the interface on the substrate surface, since the energy barrier for heterogeneous nucleation is lower than for homogeneous nucleation.

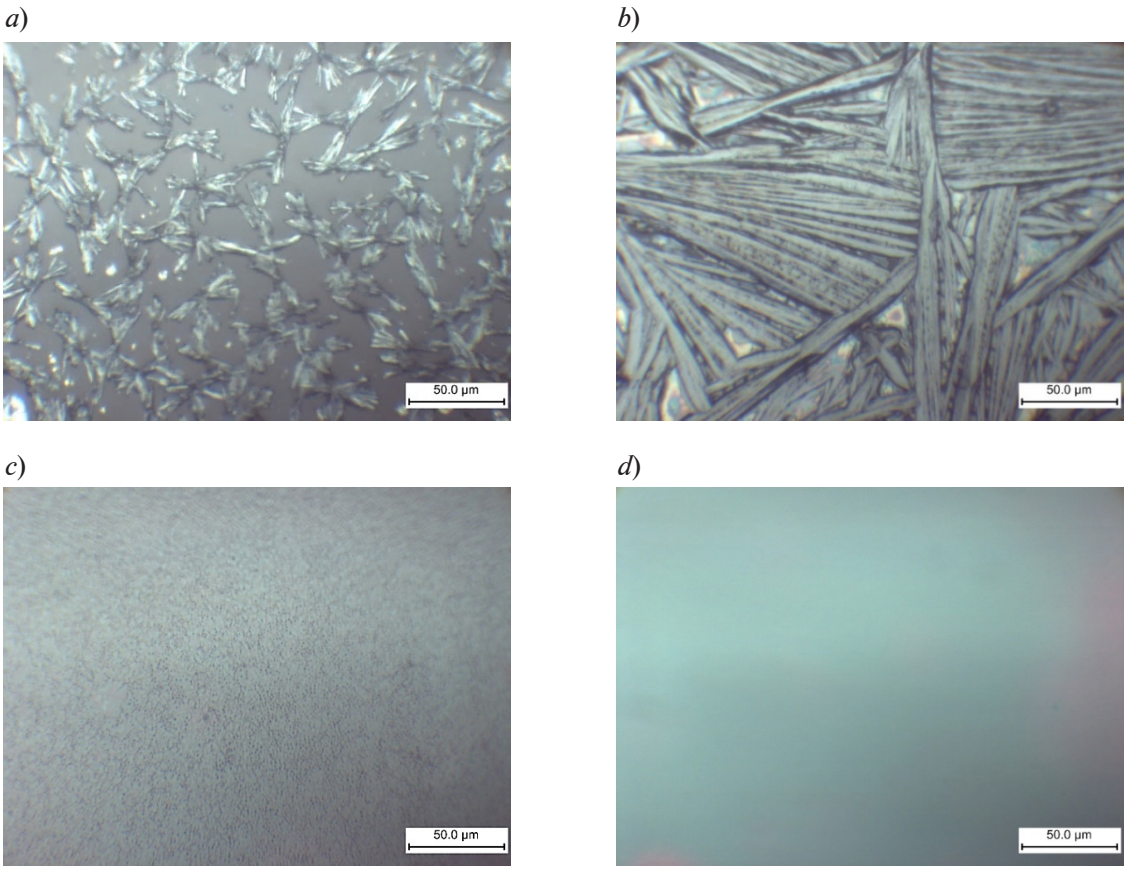

Fig. 4. Micrographs of $MA_xMEA_{1-x}PbI_3$ solid solutions obtained by one-step spin-coating from DMFA and DMSO solutions (1:4) on glass substrates: $MAPbI_3$ (*a*), $MA_{0.75}MEA_{0.25}PbI_3$ (*b*), $MA_{0.5}MEA_{0.5}PbI_3$ (*c*), $MA_{0.25}MEA_{0.75}PbI_3$ (*d*)

Analysis of AFM images of the $MAPbI_3$ coating (Fig. 5) shows the presence of small crystallites on the surface of the substrate.

For example, the observed small dark regions between large elongated crystallites in Fig. 5,*b* are crystallites formed under heterogeneous nucleation. It can be seen from Fig. 5, *c* and *d* that the size of these crystallites is tens and hundreds of nanometers. An increase in the solute concentration in the near-surface region during drying of the solution also leads to solute diffusion towards the substrate surface, while growth processes with homogeneous and heterogeneous nucleation are competing and are often observed simultaneously [23–25].

Figs. 4,*a* and 5 also show that the $MAPbI_3$ film layer contains uncoated regions of the substrate and, in general, a smaller volume of material on the substrate, while the $MA_{0.75}MEA_{0.25}PbI_3$ film completely covers the substrate even at the macroscale, and the elongated structures are much larger (see Fig. 4,*b*). This is probably due to poor wettability of the substrate surface with $MAPbI_3$ solution, which can lead to greater separation of solution droplets during spin-coating and a decrease in the volume of solution on the substrate [26]. Moreover, the lower wettability of the substrate with the solution can lead to nonuniform coating of the substrate with the formation of individual microdroplets during drying. On the other hand, a dramatic improvement in wettability of $MA_{0.75}MEA_{0.25}PbI_3$ solution with an almost twofold decrease in the contact angle by (from 20° to 12°) probably leads to an increase in the volume of the solution on the substrate during spin-coating. Nevertheless, the difference in the sizes of elongated crystallites may be related not only to the available volume of the solution, but also to a different crystallization kinetics of the $MA_{0.75}MEA_{0.25}PbI_3$ film.

As follows from the optical microscopy data for $MA_{0.5}MEA_{0.5}PbI_3$ and $MA_{0.25}MEA_{0.75}PbI_3$ films (see Fig. 4, *c*, *d*), a further decrease in the contact angle is correlated with the coating quality of the substrates with continuous and homogeneous polycrystalline layers. In this case, the

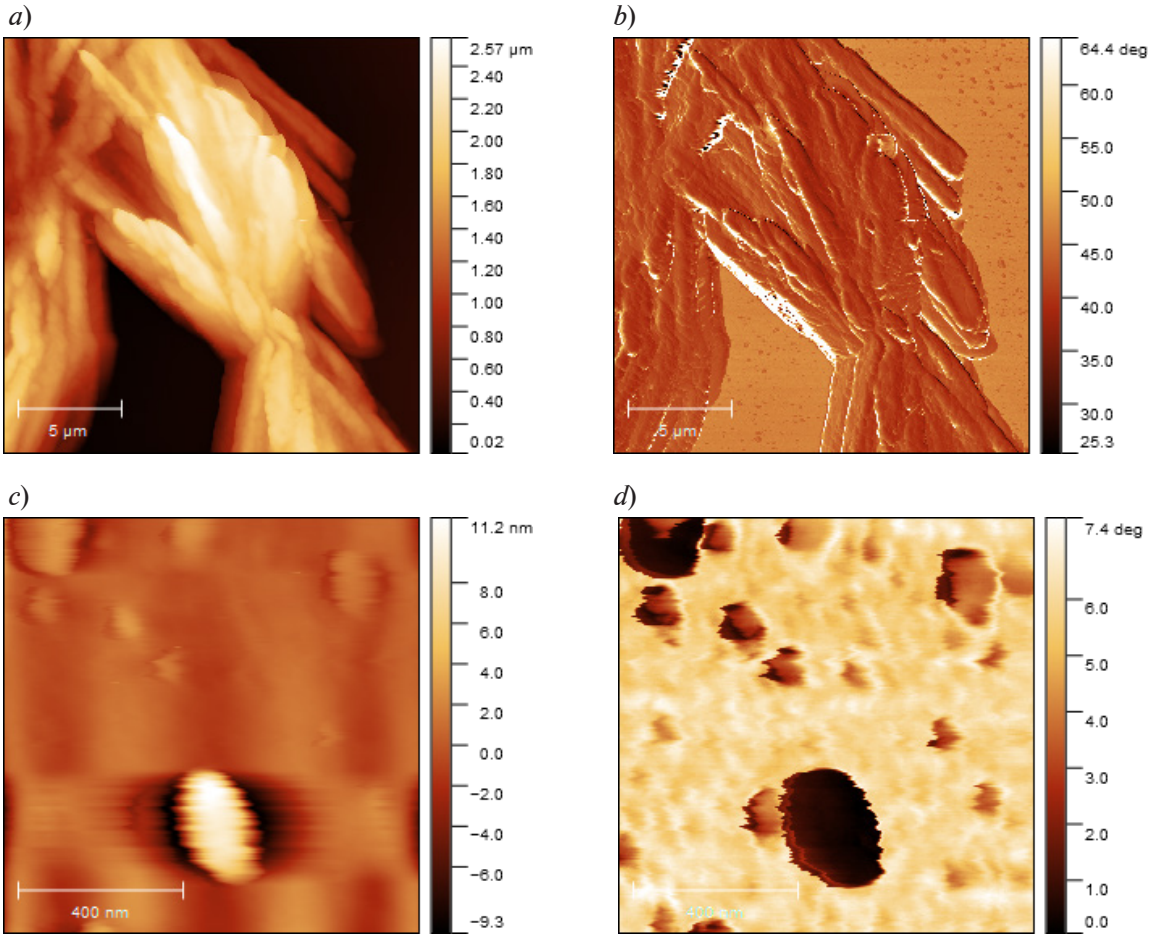

Fig. 5. AFM images of $MAPbI_3$ film: its topology (*a*, *b*) and phase contrast (*c*, *d*)

crystallization kinetics of the layer clearly changes dramatically when heterogeneous nucleation prevails, and the formation of elongated crystallites is not observed.

The contact angle for the $MA_{0.25}MEA_{0.75}PbI_3$ solution is also smaller than for the $MA_{0.5}MEA_{0.5}PbI_3$ solution. Optical microscopy studies revealed no grain boundaries or roughness for the $MA_{0.25}MEA_{0.75}PbI_3$ layer. As seen from the AFM images (Fig. 6, *a*, *b*), the $MA_{0.5}MEA_{0.5}PbI_3$ polycrystalline film demonstrates a hierarchical structure where larger grains with the approximate sizes of 0.5–1.0 μm consist of nanocrystallites with the characteristic sizes of about 50 nm. The film with a higher proportion of monoethanolammonium ($MA_{0.25}MEA_{0.75}PbI_3$) is a homogeneous coating of nanocrystallites about 50 nm in size, without forming larger grains (Fig. 6, *c*, *d*).

It was found in [27] that an increase in the wettability of the substrate surface with the solution (a decrease in the contact angle) leads to an increase in the grain concentration of the polycrystalline hybrid perovskite film. However, the change in the morphology of the films in our work cannot be explained solely by the change in the wettability of the surface with the solution, since the obtained $MA_{0.5}MEA_{0.5}PbI_3$ and $MA_{0.25}MEA_{0.75}PbI_3$ films consist of nanocrystallites of similar sizes at the nanoscale. The concentration of monoethanolammonium obviously affects the alignment of nanocrystallites in the film. This phenomenon may be related to the incorporation of monoethanolammonium not only into the crystal lattice, but also in the region at the boundaries of nanocrystallites, acting as ligand molecules limiting grain growth.

Thus, we assume that the change in the morphology of $MA_xMEA_{1-x}PbI_3$ films is due to both a change in the contact angle of the solutions (and, probably, the solvent evaporation and supersaturation rates) and to mutual alignment of the nanocrystallites of the film depending on the concentration of monoethanolammonium at the boundaries of the nanocrystallites. Thus, continuous coating of the substrate with elongated split crystallites ensures a significant change in the contact angle relative to the $MAPbI_3$ solution for the $MA_{0.75}MEA_{0.25}bI_3$ film, in contrast to

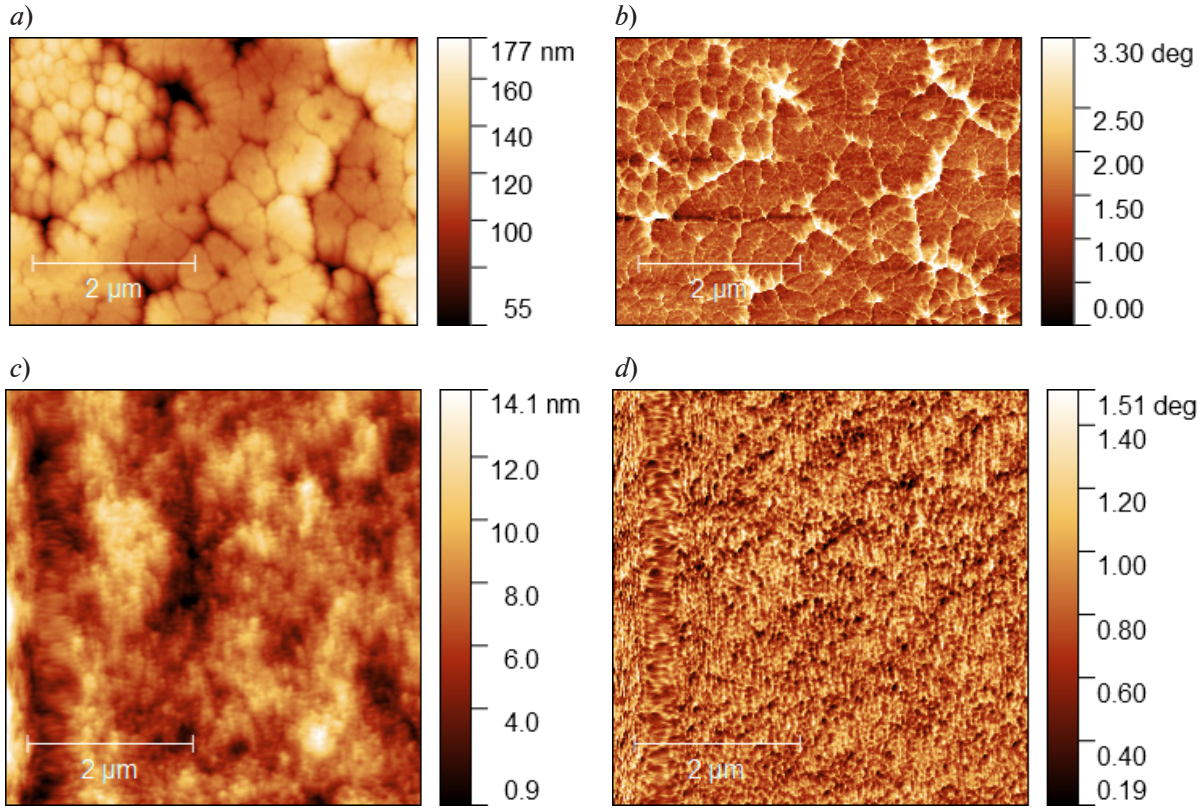

Fig. 6. AFM images of $MA_{0.5}MEA_{0.5}PbI_3$ (*a*, *b*) and $MA_{0.25}MEA_{0.75}PbI_3$ (*c*, *d*) films, showing their topology (*a*, *c*) and phase contrast (*b*, *d*)

discontinuous coating for the $MAPbI_3$ solution. However, the absence of elongated crystallites in $MA_{0.5}MEA_{0.5}PbI_3$ and $MA_{0.25}MEA_{0.75}PbI_3$ films may be due not only to violation of the conditions for homogeneous nucleation and growth of elongated crystallites due to a decrease in the contact angle, evaporation rate, and predominance of the heterogeneous nucleation mechanism, but also to a restriction of crystallite intergrowth during the incorporation of monoethanolammonium molecules at the boundaries of nanocrystallites. Nevertheless, good wettability of the substrates with $MA_{0.5}MEA_{0.5}PbI_3$ and $MA_{0.25}MEA_{0.75}PbI_3$ solutions obviously ensures good uniformity and continuity of the films without additional activation of the substrate surface.

A change in the optical absorption spectra with an increase in the band gap and a shift in XRD peaks clearly indicates the incorporation of monoethanolammonium cations into the crystal lattice in the entire range of compositions studied. Therefore, we assume that monoethanolammonium molecules are incorporated simultaneously both in the crystal lattice, forming a solid solution, and at the boundary of nanocrystallites. Notably, the $MEAPbI_3$ film did not exhibit a crystalline phase of perovskite according XRD analysis. This indicates that the incorporation of monoethanolammonium into the crystal lattice is energetically unfavorable and indirectly confirms our assumption about the possible incorporation of monoethanolammonium at the boundaries of $MA_{0.25}MEA_{0.75}PbI_3$nanocrystallites as well.

Conclusion

We considered the morphological features of polycrystalline films of hybrid perovskites $MA_xMEA_{1-x}PbI_3$, prepared by one-step spin-coating from DMF and DMSO (4:1) solutions.

The experiments indicate that an increase in the proportion of monoethanolammonium in $MA_xMEA_{1-x}PbI_3$ leads not only to a change in the absorption spectra with an increase in the band gap and interplanar distances of the crystal lattice, but also to a significant change in the morphology of the films, as well as to an improvement in wettability of $MA_xMEA_{1-x}PbI_3$ solutions. A decrease in the contact angle of $MA_xMEA_{1-x}PbI_3$ solutions with an increase in the proportion of MEA ensures the continuity of the substrate coating without additional surface activation.

Importantly, the increased band gap of $MA_xMEA_{1-x}PbI_3$ films, compared with $MAPbI_3$, makes these hybrid perovskites attractive for use in tandem solar cells. It was found that films with the composition $MA_{0.75}MEA_{0.25}PbI_3$ form elongated split crystallites with characteristic sizes of 0.1–0.2 mm under these growth conditions, which promises new avenues for the creation of photodetectors or X-ray detectors.

A further increase in the proportion of monoethanolammonium in $MA_xMEA_{1-x}PbI_3$ hybrid perovskites leads to a change in the mechanisms of film crystallization, inhibiting the growth of elongated crystallites and yielding high-quality layers for use in vertical structures such as tandem solar cells. We assume that the change in crystallization mechanisms is due not so much to a change in wettability and the predominance of heterogeneous nucleation over homogeneous nucleation, but rather to incorporation of part of the monoethanolammonium molecules at the nanocrystallite boundaries of the film.

The nature of such a phenomenon as predominant incorporation of monoethanolammonium molecules into the crystal lattice or on nanocrystallite boundaries in the film requires further research, presenting not only practical but also purely scientific interest.

REFERENCES

1. **Krishna B. G., Ghosh, D. S., Tiwari S.,** Progress in ambient air-processed perovskite solar cells: Insights into processing techniques and stability assessment, Sol. Energy. 224 (Aug) (2021) 1369–1395.

2. **Lian Z., Yan Q., Lv Q., et al.,** High-performance planar-type photodetector on (100) facet of $MAPbI_3$ single crystal, Sci. Rep. 5 (13 Nov) (2015) 16563.

3. **Kim Y. C., Kim K. H., Son D.-Y., et al.,** Printable organometallic perovskite enables large-area, low-dose X-ray imaging, Nature. 550 (7674) (2017) 87–91.

4. **Zhao X., Xu H., Wang Z., et al.,** Memristors with organic-inorganic halide perovskites, InfoMat. 1 (2) (2019) 183–210.

5. **Zhu X., Lee J., Lu W.,** Iodine vacancy redistribution in organic–inorganic halide perovskite films and resistive switching effects, Adv. Mater. 29 (29) (2017) 1700527.

6. **Bencherif H., Meddour F., Elshorbagy M. H., et al.,** Performance enhancement of $(FAPbI_3)_{1-x}(MAPbBr_3)_x$ perovskite solar cell with an optimized design, Micro Nanostructures. 171 (Nov) (2022) 207403.

7. **Gao B., Meng J.,** $RbCs(MAFA)PbI_3$ perovskite solar cell with 22.81% efficiency using the precise ions cascade regulation, Appl. Surf. Sci. 530 (15 Nov) (2020) 147240.

8. **Fan X.,** Advanced progress in metal halide perovskite solar cells: A review, Mater. Today Sustain. 24 (Dec) (2023) 100603.

9. **Nenashev G. V., Aleshin A. N., Ryabko A. A., et al.,** Effect of barium doping on the behavior of conductivity and impedance of organic-inorganic perovskite films, Solid State Commun. 388 (15 Sept) (2024) 115554.

10. **Khan F., Rezgui B. D., Khan M. T., Al-Sulaiman F. A.,** Perovskite-based tandem solar cells: Device architecture, stability, and economic perspectives, // Renewable & Sustainable Energy Reviews. 165 (Sept) (2022) 112553.

11. **Li H., Zhang W.,** Perovskite tandem solar cells: From fundamentals to commercial deployment, Chem. Rev. 120 (18) (2020) 9835–9950.

12. **Khatoon S., Yadav S. K., Chakraborty V., et al.,** Perovskite solar cell's efficiency, stability and scalability: A review, Mater. Sci. Energy Technol. 6 (1) (2023) 437–459.

13. **Kozodayev D. A., Muratova E. N., Moshnikov V. A.,** Ot nanotekhnologii k nanoarkhitektonike [From nanotechnology to architektoniks], The 79-th Scientific and Technical Conference of St. Petersburg's STS REC named after Popov, dedicated to the Day of Radio, April 22–26, 2024; ETU "LETI", Book of reports. St. Petersburg. Section 9. 1(79) (2024) 350–352.

14. **Su K., Chen W., Huang Y., et al.,** In situ graded passivation via porphyrin derivative with enhanced photovoltage and fill factor in perovskite solar cells, Solar RRL. 6 (4) (2022) 2270041.

15. **Feng W., Tan Y., Yang M., et al.,** Small amines bring big benefits to perovskite-based solar cells and light-emitting diodes, Chem. 8 (2) (2022) 351–383.

16. **Azmi R., Ugur E., Seitkhan A., et al.,** Damp heat–stable perovskite solar cells with tailored-dimensionality 2D/3D heterojunctions, Science. 376 (6588) (2022) 73–77.

17. **Leung T. L., Ahmad I., Syed A. A., et al.,** Stability of 2D and quasi-2D perovskite materials and devices, Commun. Mater. 3 (06 Sept) (2022) 63 (2022).

18. **Liu D., Li Q., Wu K.,** Ethylammonium as an alternative cation for efficient perovskite solar cells from first-principles calculations, RSC Adv. 9 (13) (2019) 7356–7361.

19. **Fan P., Gu D., Liang G., et al.,** High-performance perovskite $CH_3NH_3PbI_3$ thin films for solar cells prepared by single-source physical vapour deposition, Sci. Rep. 6 (18 July) (2016) 29910.

20. **Ryabko A. A., Ovezov M. K., Maksimov A. I., et al.,** Competing growth mechanisms during the formation of a $MAPbI_3$ polycrystalline film, Vestnik of Yaroslav the Wise Novgorod State University. (3(132)) (2023) 365–373 (in Russian).

21. **Li Y., Li X., Qianqian C., et al.,** Tuning nucleation sites to enable monolayer perovskite films for highly efficient perovskite solar cells, Coatings. 8 (11) (2018) 408.

22. **Kumar J., Srivastava P., Bag M.,** Advanced strategies to tailor the nucleation and crystal growth in hybrid halide perovskite thin films, Front. Chem. 10 (13 Apr) (2022) 842924.

23. **Moshnikov V., Muratova E., Aleshin A., et al.,** Controlled crystallization of hybrid perovskite films from solution using prepared crystal centers, Crystals. 14 (4) (2024) 376.

24. **Kim N. K., Kang D. H., Kang H. W.,** Unevenness of thin liquid layer by contact angle variation of substrate during coating process, Coatings. 9 (3) (2019) 162.

25. **Pylnev M., Barbisan A. M., Wei T.-C.,** Effect of wettability of substrate on metal halide perovskite growth, Appl. Surf. Sci. 541 (1 March) (2021) 148559.

СПИСОК ЛИТЕРАТУРЫ

1. **Krishna B. G., Ghosh, D. S., Tiwari S.** Progress in ambient air-processed perovskite solar cells: Insights into processing techniques and stability assessment // Solar Energy. 2021. Vol. 224. August. Pp. 1369–1395.

2. **Lian Z., Yan Q., Lv Q., Wang Y., Liu L., Zhang L., Pan S., Li Q., Wang L.-D., Sun J.-L.** High-performance planar-type photodetector on (100) facet of $MAPbI_3$ single crystal // Scientific Reports. 2015. Vol. 5. 13 November. P. 16563.

3. **Kim Y. C., Kim K. H., Son D.-Y., Jeong D.-N., Seo J.-Y., Choi Y. S., Han I. T., Lee S. Y., Park, N.-G.** Printable organometallic perovskite enables large-area, low-dose X-ray imaging // Nature. 2017. Vol. 550. No. 7674. Pp. 87–91.

4. **Zhao X., Xu H., Wang Z., Lin Y., Liu Y.** Memristors with organic-inorganic halide perovskites // InfoMat. 2019. Vol. 1. No. 2. Pp. 183–210.

5. **Zhu X., Lee J., Lu W.** Iodine vacancy redistribution in organic–inorganic halide perovskite films and resistive switching effects // Advanced Materials. 2017. Vol. 29. No. 29. P. 1700527.

6. **Bencherif H., Meddour F., Elshorbagy M. H., Hossain M. K., Cuadrado A., Abdi M. A., Bendib T., Kouda S., Alda J.** Performance enhancement of $(FAPbI_3)_{1-x}(MAPbBr_3)_x$ perovskite solar cell with an optimized design // Micro and Nanostructures. 2022. Vol. 171. November. P. 207403.

7. **Gao B., Meng J.** $RbCs(MAFA)PbI_3$ perovskite solar cell with 22.81% efficiency using the precise ions cascade regulation // Applied Surface Science. 2020. Vol. 530. 15 November. P. 147240.

8. **Fan X.** Advanced progress in metal halide perovskite solar cells: A review// Materials Today Sustainability. 2023. Vol. 24. December. P. 100603.

9. **Nenashev G. V., Aleshin A. N., Ryabko A. A., Shcherbakov I. P., Moshnikov V. A., Muratova E. N., Kondratev V. M., Vrubblevsky I. A.** Effect of barium doping on the behavior of conductivity and impedance of organic-inorganic perovskite films // Solid State Communications. 2024. Vol. 388. 15 September. P. 115554.

10. **Khan F., Rezgui B. D., Khan M. T., Al-Sulaiman F. A.** Perovskite-based tandem solar cells: Device architecture, stability, and economic perspectives // Renewable & Sustainable Energy Reviews. 2022. Vol. 165. September. P. 112553.

11. **Li H., Zhang W.** Perovskite tandem solar cells: From fundamentals to commercial deployment // Chemical Reviews. 2020. Vol. 120. No. 18. Pp. 9835–9950.

12. **Khatoon S., Yadav S. K., Chakraborty V., Singh J., Singh R. B., Hasnain M. S., Hasnain S. M. M.** Perovskite solar cell's efficiency, stability and scalability: A review // Materials Science for Energy Technologies. 2023. Vol. 6. No. 1. Pp. 437–459.

13. **Козодаев Д. А., Муратова Е. Н., Мошников В. А.** От нанотехнологии к наноархитектонике // 79-я Научно-техническая конференция Санкт-Петербургского НТО РЭС им. А. С. Попова, посвященная Дню радио. Сборник докладов. 22–26 апреля 2024 г., СПбГЭТУ «ЛЭТИ». Санкт-Петербург. Секция 9. № 1 (79). С. 350–352.

14. **Su K., Chen W., Huang Y., Yang G., Brooks K. G., Zhang B., Feng Y., Nazeeruddin M. K., Zhang Y.** In situ graded passivation via porphyrin derivative with enhanced photovoltage and fill factor in perovskite solar cells // Solar RRL. 2022. Vol. 6. No. 4. P. 2270041.

15. **Feng W., Tan Y., Yang M., Jiang Y., Lei B.-X., Wang L. P., Wu W.-Q.** Small amines bring big benefits to perovskite-based solar cells and light-emitting diodes // Chem. 2022. Vol. 8. No. 2. Pp. 351–383.

16. **Azmi R., Ugur E., Seitkhan A., et al.** Damp heat–stable perovskite solar cells with tailored-dimensionality 2D/3D heterojunctions // Science. 2022. Vol. 376. No. 6588. Pp. 73–77.

17. **Leung T. L., Ahmad I., Syed A. A., Ng A. M. C., Popović J., Chen W.** Stability of 2D and quasi-2D perovskite materials and devices // Communications Materials. 2022. Vol. 3. 06 September. P. 63 (2022).

18. **Liu D., Li Q., Wu K.** Ethylammonium as an alternative cation for efficient perovskite solar cells from first-principles calculations // Royal Society of Chemistry
(RSC) Advances. 2019. Vol. 9. No. 13. Pp. 7356–7361.

19. **Fan P., Gu D., Liang G., Luo J., Chen J.-L., Zheng Z., Zhang D.** High-performance perovskite $CH_3NH_3PbI_3$ thin films for solar cells prepared by single-source physical vapour deposition // Scientific Reports. 2016. Vol. 6. 18 July. P. 29910.

20. **Рябко А. А., Овезов М. К., Максимов А. И., Алешин А. М., Мошников В. А.** Конкурирующие механизмы роста при формировании поликристаллической пленки $MAPbI_3$ // Вестник Новгородского государственного университета. 2023. № 3 (132) С. 365–373.

21. **Li Y., Li X., Qianqian C., Dong H., Yao J.-T., Zhou Y., Yang G.-J.** Tuning nucleation sites to enable monolayer perovskite films for highly efficient perovskite solar cells // Coatings. 2018. Vol. 8. No. 11. P. 408.

22. **Kumar J., Srivastava P., Bag M.** Advanced strategies to tailor the nucleation and crystal growth in hybrid halide perovskite thin films // Frontiers in Chemistry. 2022. Vol. 10. 13 April. P. 842924.

23. **Moshnikov V., Muratova E., Aleshin A., Maksimov A., Nenashev G., Vrublevsky I., Lushpa N., Tuchkovsky A., Zhilenkov A., Kichigina O.** Controlled crystallization of hybrid perovskite films from solution using prepared crystal centers // Crystals. 2024. Vol. 14. No. 4. P. 376.

24. **Kim N. K., Kang D. H., Kang H. W.** Unevenness of thin liquid layer by contact angle variation of substrate during coating process // Coatings. 2019. Vol. 9. No. 3. P. 162.

25. **Pylnev M., Barbisan A. M., Wei T.-C.** Effect of wettability of substrate on metal halide perovskite growth // Applied Surface Science. 2021. Vol. 541. 1 March. P. 148559.

THE AUTHORS

RYABKO Andrey A.
Ioffe Institute of RAS
26 Polytekhnicheskaya St., St. Petersburg, 194021, Russia
a.a.ryabko93@yandex.ru
ORCID: 0000-0001-9626-7612

OVEZOV Maksat K.
Ioffe Institute of RAS
26 Polytekhnicheskaya St., St. Petersburg, 194021, Russia
strontiumx94@gmail.com
ORCID: 0009-0009-6273-1478

MAXIMOV Alexander I.
St. Petersburg Electrotechnical University "LETI"
5 Professor Popov St., St. Petersburg, 197376, Russia
aimaximov@mail.ru
ORCID: 0000-0003-0195-8870

PERMIAKOV Nikita V.
St. Petersburg Electrotechnical University "LETI"
5 Professor Popov St., St. Petersburg, 197376, Russia
nvpermiakov@etu.ru
ORCID: 0000-0002-6953-9958

TUCHKOVSKIY Alexander K.
Belarusian State University of Informatics and Radioelectronics
6 Petrus Brovka St., Minsk, 220013, Republic of Belarus
a.tuchkovskij@bsuir.by

VRUBLEVSKIY Igor A.
Belarusian State University of Informatics and Radioelectronics
6 Petrus Brovka St., Minsk, 220013, Republic of Belarus
vrublevsky@bsuir.edu.by
ORCID: 0000-0002-6796-8994

MURATOVA Ekaterina N.
St. Petersburg Electrotechnical University "LETI"
5 Professor Popov St., St. Petersburg, 197376, Russia
sokolovaeknik@yandex.ru
ORCID: 0000-0002-4181-6669

ALESHIN Andrey N.
Ioffe Institute of RAS
26 Polytekhnicheskaya St., St. Petersburg, 194021, Russia
aleshin.transport@mail.ioffe.ru
ORCID: 0000-0001-5449-4446

MOSHNIKOV Vyacheslav A.
St. Petersburg Electrotechnical University "LETI"
5 Professor Popov St., St. Petersburg, 197376, Russia
vamoshnirov@mail.ru
ORCID: 0000-0001-6500-5492

СВЕДЕНИЯ ОБ АВТОРАХ

РЯБКО Андрей Андреевич – *кандидат технических наук, младший научный сотрудник лаборатории неравновесных процессов в полупроводниках Физико-технического института имени А. Ф. Иоффе РАН.*
194021, Россия, г. Санкт-Петербург, Политехническая ул., 26
a.a.ryabko93@yandex.ru
ORCID: 0000-0001-9626-7612

ОВЕЗОВ Максат Кемалович – *младший научный сотрудник лаборатории неравновесных процессов в полупроводниках Физико-технического института имени А. Ф. Иоффе РАН.*
194021, Россия, г. Санкт-Петербург, Политехническая ул., 26
strontiumx94@gmail.com
ORCID: 0009-0009-6273-1478

МАКСИМОВ Александр Иванович – кандидат *физико-математических наук, доцент кафедры микро- и наноэлектроники Санкт-Петербургского государственного электротехнического университета «ЛЭТИ» имени В. И. Ульянова (Ленина).*
197376, Россия, г. Санкт Петербург, ул. Проф. Попова, 5
aimaximov@mail.ru
ORCID: 0000-0003-0195-8870

ПЕРМЯКОВ Никита Вадимович – *доцент кафедры микро- и наноэлектроники Санкт-Петербургского государственного электротехнического университета «ЛЭТИ» имени В. И. Ульянова (Ленина).*
197376, Россия, г. Санкт Петербург, ул. Проф. Попова, 5
nvpermiakov@etu.ru
ORCID: 0000-0002-6953-9958

ТУЧКОВСКИЙ Александр Константинович – *старший научный сотрудник Белорусского государственного университета информатики и радиоэлектроники.*
220013, Республика Беларусь, г. Минск, ул. Петруся Бровки, 6
a.tuchkovskij@bsuir.by
ORCID: --

ВРУБЛЕВСКИЙ Игорь Альфонсович – *доцент Белорусского государственного университета информатики и радиоэлектроники.*
220013, Республика Беларусь, г. Минск, ул. Петруся Бровки, 6
vrublevsky@bsuir.edu.by
ORCID: 0000-0002-6796-8994

МУРАТОВА Екатерина Николаевна – *доцент кафедры микро- и наноэлектроники Санкт-Петербургского государственного электротехнического университета «ЛЭТИ» имени В. И. Ульянова (Ленина).*
197376, Россия, г. Санкт Петербург, ул. Проф. Попова, 5
sokolovaeknik@yandex.ru
ORCID: 0000-0002-4181-6669

АЛЕШИН Андрей Николаевич – *доктор физико-математических наук, заведующий лабораторией неравновесных процессов в полупроводниках Физико-технического института имени А. Ф. Иоффе РАН.*
194021, Россия, г. Санкт-Петербург, Политехническая ул., 26
aleshin.transport@mail.ioffe.ru
ORCID: 0000-0001-5449-4446

МОШНИКОВ Вячеслав Алексеевич – *доктор физико-математических наук, профессор кафедры микро- и наноэлектроники Санкт-Петербургского государственного электротехнического университета «ЛЭТИ» имени В. И. Ульянова (Ленина).*
197376, Россия, г. Санкт Петербург, ул. Проф. Попова, д. 5
vamoshnirov@mail.ru
ORCID: 0000-0001-6500-5492

Статья поступила в редакцию 28.09.2024. Одобрена после рецензирования 04.12.2024. Принята 04.12.2024.
Received 28.09.2024. Approved after reviewing 04.12.2024. Accepted 04.12.2024.